NEOPLASIA
www.neoplasia.com

Volume 21 Number 4 April 2019 pp. 363–375 363

Blocking Mitotic Exit of Ovarian Cancer Cells by Pharmaceutical Inhibition of the Anaphase-Promoting Complex Reduces Chromosomal Instability

Monika Raab[*], Mourad Sanhaji[*], Shengtao Zhou[†], Franz Rödel[‡,§], Ahmed El-Balat[*], Sven Becker[*] and Klaus Strebhardt[*,§]

[*]Department of Gynecology, Goethe-University, Frankfurt am Main; [†]State Key Laboratory of Biotherapy, Department of Obstetrics and Gynecology, West China Second Hospital, Sichuan University, Chengdu, 610041, P. R. China; [‡]Department of Radiotherapy and Oncology, Goethe University; [§]German Cancer Consortium (DKTK) / German Cancer Research Center, partner site, Frankfurt a. M.

Abstract

Paclitaxel is a frontline drug for the treatment of epithelial ovarian cancer (EOC). However, following paclitaxel-platinum based chemotherapy, tumor recurrence occurs in most ovarian cancer patients. Chromosomal instability (CIN) is a hallmark of cancer and represents genetic variation fueling tumor adaptation to cytotoxic effects of anticancer drugs. In this study, our Kaplan-Meier analysis including 263 ovarian cancer patients (stages I/II) revealed that high Polo-like kinase (PLK) 1 expression correlates with bad prognosis. To evaluate the role of PLK1 as potential cancer target within a combinatorial trial, we induced strong mitotic arrest in ovarian cancer cell lines by synergistically co-targeting microtubules (paclitaxel) and PLK1 (BI6727) followed by pharmaceutical inhibition of the Anaphase-Promoting Complex (APC/C) using proTAME. In short- and long-term experiments, this triple treatment strongly activated apoptosis in cell lines and primary ovarian cells derived from cancer patients. Mechanistically, BI6727/paclitaxel/proTAME stabilize Cyclin B1 and trigger mitotic arrest, which initiates mitochondrial apoptosis by inactivation of antiapoptotic BCL-2 family proteins, followed by activation of caspase-dependent effector pathways. This triple treatment prevented endoreduplication and reduced CIN, two mechanisms that are associated with aggressive tumors and the acquisition of drug resistance. This "two-punch strategy" (strong mitotic arrest followed by blocking mitotic exit) has important implications for developing paclitaxel-based combinatorial treatments in ovarian cancer.

Neoplasia (2019) 21, 363–375

Introduction

Epithelial ovarian cancer (EOC) is a leading cause of cancer death in women worldwide [1,2]. Microtubule targeting inhibitors like paclitaxel represent one of the most important and promising classes of cancer drugs used in the treatment of ovarian, breast, and lung cancer [3,4]. The Gynecological Cancer Inter Group recommended in 2005 as standard of care for first-line chemotherapy the intravenous administration of paclitaxel in combination with carboplatin every 3 weeks for 6 cycles [5,6]. Approximately two-thirds of ovarian cancer patients will respond to a therapeutical strategy that starts with surgical debulking and is followed by a paclitaxel/carboplatin-including chemotherapy, but tumor recurrence occurs in most patients at a median of 15 months from initial diagnosis [7–9] often followed by chemoresistance. In addition to its role as first-line agent in a combined therapy, paclitaxel is a promising agent for relapsed platinum-refractory epithelial ovarian cancer. However, the response to microtubule targeting agents is highly variable, which might interfere with clinical efficiency [10–12]. Importantly, while certain side effects like myelosuppression are manageable, more problematic are the peripheral neuropathies induced by inhibiting microtubule dynamics in nondividing cells [13].

Abbreviations: CIN, chromosomal instability; APC/C, Anaphase-Promoting Complex; EOC, epithelial ovarian cancer; PLK1, polo-like kinase 1

Address all correspondence to: Prof. Dr. K. Strebhardt, Department of Gynecology, Goethe-University, Theodor-Stern-Kai 7, 60590 Frankfurt am Main.

Received 17 January 2019; Accepted 29 January 2019

1476-5586
https://doi.org/10.1016/j.neo.2019.01.007

Paclitaxel treatment arrests cells in mitosis due to the presence of a small number of unattached kinetochores [14], which have not made stable attachments to microtubules, thereby activating the spindle assembly checkpoint (SAC) that delays mitotic progression by inhibiting the ubiquitin ligase activity of the anaphase-promoting complex/cyclosome (APC/C) [15–17]. The APC/C represents a highly complex ubiquitin ligase machinery. At different cell cycle stages the activator proteins CDH1 and CDC20 associate with certain subunits of the APC/C to stimulate APC/C-dependent ubiquitination of substrates and their subsequent proteolysis by the 26S proteasome [18]. Furthermore, the exit from mitosis and the onset of anaphase require CDC20-dependent ubiquitination of APC/C substrates including securin and mitotic cyclins. Cyclin B1 is one of the most important substrates of the APC/C that plays a key role for the timing of the mitotic arrest.

Recently, pharmacological inhibitors of the APC/C called proTAME and apcin [19,20] have been developed. Within living cells, the small molecule inhibitor proTAME, which is a cell-permeable prodrug, is converted to TAME (Tosyl-L-Arginine Methyl Ester) by intracellular esterases. The three-dimensional conformation of TAME resembles the isoleucine/arginine tail of the activator proteins CDH1 and CDC20 and has therefore the ability to bind to the APC/C, preventing the association of CDH1 or CDC20 with the APC/C [20].

Polo-like kinase 1 (PLK1) regulates multiple steps of the cell-cycle progression [21–23]. The inhibition of PLK1, like the deregulation of microtubule dynamics by paclitaxel, activates the SAC. PLK1 is overexpressed in multiple cancer types including ovarian cancer [24–30]. Interestingly, PLK1 overexpression correlates with bad prognosis in various types of cancer patients [24,31–33]. Remarkably, high PLK1 levels have also been associated with a high risk of metastases, indicating a role for PLK1 in more malignant tumors. Numerous studies using xenograft models revealed PLK1 as a very attractive cancer target [34–37]. Volasertib (BI6727) is the most advanced clinical PLK1 inhibitor. A significant correlation between PLK1-positive cells and the histological grade of ovarian cancer was observed [38]. An investigation on benign and tumor tissues derived from human ovaries revealed that the frequency of PLK1 expression was low in normal ovarian epithelium and borderline tumors, but a high frequency was observed in 26% of ovarian cancer tissues [30]. In a recent study, a similar antitumor activity in patients with ovarian cancer was shown comparing Volasertib (BI6727) targeting PLK1 and a single-agent chemotherapy, e.g., paclitaxel [39]. However, the precise roles of PLK1 as prognostic marker and as therapeutic target in early stage ovarian cancer remain elusive.

Cells arrested in mitosis by paclitaxel or by the PLK1 inhibitor BI6727 can enter an apoptotic pathway during mitosis or execute mitotic slippage, thereby entering G1 without undergoing anaphase or cytokinesis to end up as single, tetraploid cell [40]. Following slippage, cells can arrest, cycle, or die after slippage [41]. The cellular factors that determine the outcome of mitotic arrest currently remain unknown. A recent study has shown that preventing mitotic slippage by downregulating CDC20 via RNAi may increase the sensitivity of tumor cells to microtubule-targeting agents [42]. In EOC cells, little is known about the APC/C and its co-activator CDC20. In this study, we first studied the prognostic relevance of PLK1 in a cohort of 263 ovarian cancer patients (stages I/II). Moreover, we aimed to elucidate the importance and therapeutic potential of small molecule inhibitors of the APC/C in EOC cells mitotically arrested by paclitaxel and a clinical PLK inhibitor.

Materials and Methods

Patients Characteristics (Immunohistochemistry)

Following an institutional review board approval (Institutional Ethics Committee of Sichuan University, Ethics approval no. 20180928032) and after obtaining written informed consent, a total of 293 patients with ovarian carcinoma were included in this study. Our study conforms to the guidelines set by the Declaration of Helsinki. The median age was 51 years with a range of 34 years to 85 years. Seventy-one patients presented with stage I (24.2%) and 222 patients (75.8%) presented with stage II disease. A total of 285 patients (97.3%) were of serous and 8 patients (2.7%) of a mixed pathological subtype; 283 patients (96.6%) displayed a low- and 10 patients (3.4%) a moderate-grade differentiation. Median follow-up for all patients was 30 months (range: 1-109 months).

Scoring for PLK1 Expression

Production of tissue microarrays of ovarian cancer specimens was generated from West China Second Hospital, Sichuan University. All those patients included have not received chemotherapy prior to surgery, and at least two independent pathologists have examined the accuracy of the pathological diagnosis in a double-blinded manner. Slices were subject to a standardized horseradish peroxidase technique with primary anti-PLK1 antibodies (Santa Cruz Biotechnology) at a 1:100 dilution. Next, dextran polymer-conjugated horseradish peroxidase and 3,3-diaminobenzidine chromogen were utilized for visualization followed by counterstaining with hematoxylin solution. PLK1 immunoreactivity was evaluated semiquantitatively by two independent investigators (F.R. and M.S.) without knowledge of the patients' clinicopathologic and clinical characteristics considering both the percentage of positive tumor cells [1 (0%-25%), 2 (26%-50%), 3 (51%-75%), and 4 (> 75%)] and the intensity of staining scored as 1+ (weak), 2+ (moderate), and 3+ (intense). These parameters were multiplied to produce an individual weighted score (WS). To facilitate further statistical analysis, the histochemical sores were arbitrarily dichotomized: A WS ≤ 6 was classified as "low" and a WS of >6 was classified as "high" PLK1 expression. Overall survival was defined as the time of surgical tumor resection to death by ovarian cancer by any reasons or the day of the last follow-up. Survival curves were plotted according to the method of Kaplan-Meier. Statistical analysis was performed using IBM SPSS software version 25.

Patients and Samples (Primary Cell Culture)

This study was conducted according to the "REporting recommendations for tumor MARKer prognostic studies" [43]. To establish primary, patient-derived ovarian cancer cell cultures, we analyzed samples from patients undergoing surgical resection between January 2015 and March 2018 at the Department of Gynecology of the Goethe University Hospital in Frankfurt am Main, Germany. For the samples with validated diagnosis, sufficient archival material for immunohistochemical analysis was available. The Local Research Ethics Committees approved studies of human tissue, and samples were processed anonymously.

Antibodies and Chemicals

Primary antibodies were obtained from the following sources: PLK1 (05-844), phospho-Histone H3 (Ser10) (05806) from Millipore; Cyclin B1 (GNS1), Cyclin A (B-8), CDC27 (AF 3.1), and p55CDC20 (H-175) from Santa Cruz; PARP (9542), cleaved PARP (9542), Caspase-3 (9668), and cleaved Caspase-3 (8610) from Cell Signaling; MCL-1 (ADI-AAP-240-D) from Enzo; Securin (ab3305) and BCL-X_L pS62 (ab30655) from Abcam; and from Santa Cruz; BCL-2 (7) from BD Transduction. β-Actin (A2228-100UL) from Sigma-Aldrich served as loading control.

Secondary antibodies for western blot analysis against rabbit (NA934V) and mouse (NXA931) IgG were obtained from GE Healthcare. Secondary antibodies used for immunofluorescence staining were obtained from Dako (F0313). Reagents were purchased from the following sources: Paclitaxel (T7402) Sigma-Aldrich, BI6727 (BYT-ORB181049) Selleckchem, propidium iodide (440300250) Acros Organics, RNase A (1007885) Qiagen, PE Annexin V (556421) and 7AAD (21-68981E) BD Biosciences, proTAME (1–440) Boston Biochem.

Western Blot Analysis

Protein extracts of cells were prepared by lysis in RIPA buffer (Sigma) supplemented with protease inhibitors (Complete protease inhibitor cocktail, Roche). Protein extracts (25 µg) were separated by SDS-PAGE and transferred onto PVDF membranes using the TransBlot Turbo Transfer System (BioRad). After blocking with 5% BSA in PBS with 0.1% Tween-20 for 30 minutes, the membrane was incubated with primary antibodies for 1 hour at room temperature. HRP-linked secondary antibodies were incubated 30 minutes at room temperature followed by ECL detection (ECL Chemiluminescent Western Blot Substrate, Pierce).

Colony Formation Assay

Cells were treated with paclitaxel, BI6727, or both for 24 hours. In case of combinatorial treatments with proTAME, cells were treated first with paclitaxel/BI6727 for 24 hours followed by proTAME for 24 hours. Subsequently, 2000 cells were seeded in 6-well plates. Colonies were fixed using 70% EtOH and stained with Coomassie Brilliant Blue. The numbers of grown colonies were counted and images were taken using AxioObserver Z1 microscope (Zeiss) as well as the ChemiDoc MP system (BioRad).

Cell Culture

The ovarian carcinoma cell lines OVCAR-3 and SKOV-3 were cultured in RPMI 1640 (Gibco) and in McCoy's 5a (Gibco), respectively, both containing 10% FCS (Gibco) and 1% Penicillin/Streptomycin (Sigma-Aldrich). Primary cells were isolated from ovarian cancer tissues using the tumor dissociation kit (Max Miltenyi 130-095-929) together with the tumor cell isolation kit (Max Miltenyi 130-108-339) following the manufacturer's instructions. Isolated fibroblasts were cultured as described [44].

Three-Dimensional (3D) Cultures

A cell suspension of 3000 cells/50 µl was prepared and pipetted from the topside into a 96-well Perfect 3D Hanging Drop plate (BioTrend). Plates were incubated at 37°C for 3 days until hanging drops have developed. The 3D culture was harvested on a 96-well plate covered with 1% agarose by low-spin centrifugation. Treatment of cells with BI6727, paclitaxel, and/or proTAME was performed as indicated. Cells were stained with the LIVE/DEAD viability/cytotoxicity kit (Molecular Probes/Thermofisher) for 30 minutes and inspected using a fluorescence microscope. While the polyanionic dye calcein is retained in live cells, producing an intense uniform green fluorescence, EthD-1 enters cells with damaged membranes, thereby producing a bright red fluorescence upon binding to nucleic acids in dead cells. The ratios of viable/dead cells were calculated with the software ImageJ Fiji.

Cell Proliferation and Caspase-3/7 Activity (Multiplexed Protocol)

Forty-eight hours following transfection, 7 µl substrate of the Cell Titer-Blue Cell Viability Assay (Promega) was added to each well. After a short centrifugation step (1000 rpm for 10 seconds), cells were incubated for further 3 hours at 37°C/5% CO_2 before fluorescence reading (Victor X4, PerkinElmer). The activity of Caspase-3/7 was determined using the Caspase-Glo 3/7 Assay (Promega). Twenty microliters of substrate per well was applied, and after 30-minute shaking at room temperature in the dark, luminescence was detected (Victor X4, Perkin Elmer). The analysis of data was done online by Networkanalyst and GraphPad Prism.

Cell Cycle and Apoptosis Assays

The treatment with paclitaxel, BI6727, and/or proTAME was conducted at least for 24 hours followed by cell cycle and apoptosis measurements after predefined time intervals. For cell cycle analysis, cells were harvested, washed, fixed with 70% EtOH, and stained as described [45,46]. Cell cycle quantification was performed using a FACS Calibur and Cellquest Pro software (both BD Biosciences). The activity of Caspase-3/7 was determined in cell lysates using the Caspase-Glo 3/7 Assay according to the manufacturer's instructions.

Proliferation Assays

To measure cell proliferation using the Cell Titer-Blue Cell Viability Assay, 2500 cells per well were seeded in 96-well plates and treated with paclitaxel, BI6727, and/or proTAME. Cells were incubated with 20 µl substrate of the Cell Titer-Blue Cell Viability Assay for 4 hours, and the light absorbance was measured at 540 nm (Victor X4, Perkin Elmer). The 50% inhibitory concentration (IC_{50}) was estimated using the following formula: $100 \times (T - T0)/(C - T0) = 50$, where T is the optical density (OD) value after drug treatment, $T0$ is the OD value at time 0, and C is the OD value for the diluent treatment. Time 0 was defined as the day the drug was administered.

Time-Lapse Microscopy

Thymidine-synchronized ovarian cells expressing mCherry-histone H2B were released for 5 hours, treated either with single agents or combinations. For time-lapse analysis, the treated cells were transferred to the microscope stage, and microscopy was performed with Axioimager inverted Z1 (Zeiss) equipped with an environmental chamber (Zeiss) that maintained the cells at 37°C in a humidified environment of 5% CO_2. Images were taken every 10 minutes using an Axiocam MRm camera (Zeiss) driven by Axiovision SE64 software (Zeiss). Movies and JPEG files were imported into ImageJ and proceeded using the same software. Nuclear envelope breakdown was judged as such when the nuclear membrane lost a smooth and the linear periphery. The first frame showing a poleward movement of the chromosomes was defined as anaphase onset.

Chromosome Spreads

Cells were treated overnight with 3.3 µM Nocodazol. The next day, cells were harvested by mitotic shake off and hypotonically swollen in 40% medium/ 60% tap water for 20 minutes at 37°C. Cells were fixed with freshly made Carnoy's solution (75% methanol, 25% acetic acid), and the fixative was changed several times. For spreading, cells in Carnoy's solution were dropped onto prechilled glass slides. Slides were dried at room temperature for 24 hours and stained with DAPI. Chromosome number per condition was counted using an AxioObserver.Z1 microscope with a HCX PL APO CS 63.0x1.4 oil UV objective (Zeiss, Göttingen). The graphic representation of the results was done using GraphPad Prism software.

Statistical Analysis

All experiments were performed at least three times and displayed as mean and standard error of the mean. The statistical significance was assessed by Student's t test (two-tailed and paired) using Excel

2010 (Microsoft) as well as GraphPad Prism 7 (GraphPad, La Jolla, CA). Significant differences (*$P \leq .05$; **$P \leq .01$; ***$P \leq .001$) are indicated in the figures with asterisks.

Image Work

Images were opened in Adobe Photoshop CS6, sized, and placed in figures using Adobe Illustrator CS6 (Adobe Systems, Mountain View, CA).

Results

PLK1 Gene Expression and Survival of Ovarian Cancer Patients

At first, we studied the prognostic role of PLK1 expression in ovarian cancer patients and evaluated the correlation between PLK1 expression and patient's survival based on methods for survival analysis. One hundred sixteen patients (44.1%) had high PLK1 expression, and 147 patients (55.8%) displayed low PLK1 detection. According to a Kaplan-Meier analysis, patients in clinical stages I and II with a high PLK1 (WS> 6) expression displayed a significantly ($P = .028$) impaired overall survival (62.3 months, 95% confidence interval: 52.8-76.8) compared to those having a low PLK1 expression (75.9 months, 95% confidence interval: 68.1-83.7) (Figure 1*A*).

Small Molecule APC/C Inhibitors Decrease the Viability of Mitotically Arrested Ovarian Cancer Cells and Sensitize Cells to Paclitaxel

Considering the prognostic and potential therapeutic role of PLK1 for early- and late-stage ovarian cancer, we determined the viability of

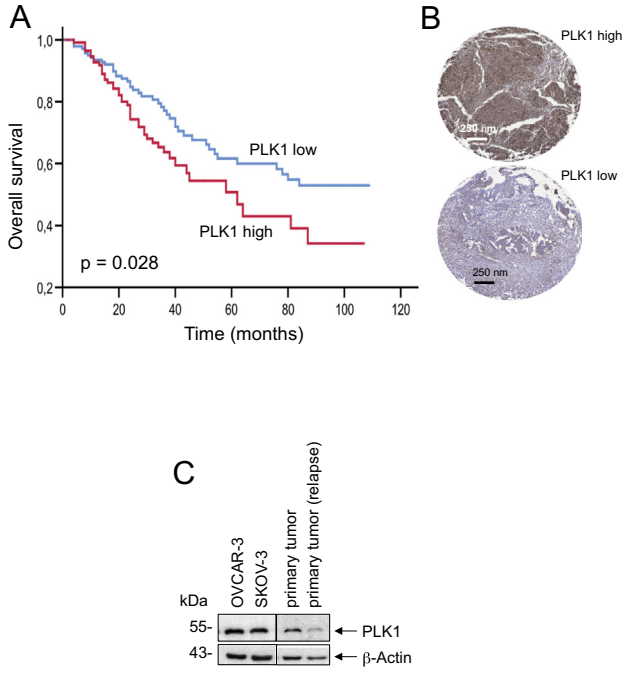

Figure 1. Kaplan-Meier analysis of ovarian cancer patients in stages I/II and examination of PLK1 expression. (A) Overall survival in 263 patients with ovarian cancer stage I and II disease according to PLK1 expression based on immunohistochemical evaluation of tumor resection specimens. (B) Representative examples of ovarian carcinoma with a low (WS ≤ 6) and high (WS> 6) detection of PLK1 in tumor cells. Original magnification × 10, scale bars 250 μm. (B) Whole cell lysates of OVCAR-3, SKOV-3, and primary ovarian cancer cells were analyzed for PLK1 expression. Endogenous levels of PLK1 and β-Actin were determined by immunoblotting.

OVCAR-3 cells expressing PLK1 (Figure 1*B*) upon treatment with the potent clinical PLK inhibitor BI6727 [47] or paclitaxel. The treatment with increasing concentrations revealed IC_{50}s of 2.75 nM for paclitaxel and 15 nM for BI6727, respectively (Supplementary Figure S1, *A* and *B*). In a combinatorial approach including 10 nM BI6727, the IC_{50} for paclitaxel dropped to 1.4 nM (Supplementary Figure S1*C*).

The antiproliferative basis for paclitaxel has long been thought to be due to the presence of an activated SAC that culminates in a mitotic cell death [40]. However, depending on the biological context and cell type, cells can escape from cell death by mitotic slippage. Thus, mitotic slippage represents a potential mechanism limiting the effectiveness of paclitaxel. To elucidate the importance and the therapeutic potential of an APC/C inhibitor that blocks exit of mitotically arrested cells induced by paclitaxel/BI6727, we tested first the effect of increasing proTAME concentrations on OVCAR-3 cells and determined the IC_{50} to be 12.5 μM (Supplementary Figure S1*D*). In addition, cells were pretreated for 24 hours with increasing concentrations of paclitaxel and 10 nM BI6727 to induce a strong mitotic arrest followed by 20 μM proTAME for additional 24 hours. The treatment with BI6727 and proTAME decreased the IC_{50} of paclitaxel further to 0.9 nM (Supplementary Figure S1*E*). In all, following combinatorial experiments including the mitotic inhibitors (paclitaxel, BI6727) and proTAME, we treated cells first with mitotic inhibitor/s for 24 hours followed by an incubation period of 24 hours with proTAME.

To investigate whether these effects are cell type-specific, we studied a second EOC cell line, SKOV-3. The treatment with increasing concentrations of paclitaxel reduced cellular viability and revealed an IC_{50} of 7 nM (Supplementary Figure S2*A*). For BI6727 an IC_{50} of 28 nM, for paclitaxel/BI6727 an IC_{50} of 2.4 nM, and for proTAME an IC_{50} of 12.5 μM were determined (Supplementary Figure S2, *B-D*). The sequential triple combination with increasing concentrations of paclitaxel and 20 nM BI6727 for 24 hours followed by 10 μM pro TAME for additional 24 hours reduced the IC_{50} for paclitaxel to 1.4 nM (Supplementary Figure S2*E*), supporting that the combinatorial treatment with a PLK1 inhibitor and proTAME reduces significantly the IC_{50} of paclitaxel in ovarian cancer cells.

The cell cycle analysis using a flow cytometer (FACS) revealed that 2.5 nM paclitaxel (24 hours) induced a small increase of OVCAR-3 cells in the G_2/M phase from 19% to 21% due to prolonged mitotic arrest as shown by microscopical inspection. The incubation with 15 nM BI6727 (24 hours) increased the fraction of cells in the G_2/M phase to 44% and the treatment with 10 μM proTAME to 26% (Supplementary Figure S3*A*). The combinatorial treatment in OVCAR-3 and SKOV-3 cells showed the most pronounced enrichment of cells in G_2/M with 62% and 78%, respectively (Supplementary Figure S3, *A* and *B*).

Blocking the APC/C Inhibits Long-Term Growth of Mitotically Arrested Ovarian Cancer Cells

To assess whether the APC/C could be a potential target to inhibit the long-term growth of ovarian cancer cells arrested in mitosis, we tested first the activity of proTAME in OVCAR-3 cells. In a co-immunoprecipitation experiment with increasing concentrations of proTAME, we could demonstrate the reduced association of CDC20 and a component of the APC/C, CDC27, in a dose-dependent manner (Figure 2*A*). Inhibiting the binding of CDC20 to the CDC27 prevents activation of the APC/C stabilizing Cyclin B1 (Figure 2*A*, upper panel), which plays an important role to keep cells arrested in mitosis.

Despite a strong impact of the triple combination on the viability after 48 hours of treatment, we determined the percentage of remaining,

still viable cells to be 20% for OVCAR-3 cells and 30% for SKOV-3 cells, respectively (Supplementary Figures S1*E* and S2*E*). Therefore, we conducted experiments to investigate the fate of ovarian cancer cells over a prolonged period of time. We inhibited the mitotic exit of paclitaxel/BI6727-treated cells by incubation with proTAME and tested the viability up to 96 hours. While single agents at concentrations of 2.5 nM paclitaxel, 10 nM BI6727, or 10 μM proTAME could not prevent an increase in cell numbers, only the combinations paclitaxel/BI6727 and paclitaxel/BI6727/proTAME reduced cell numbers significantly ($P < .001$) (Figure 2*B*). We observed the most pronounced

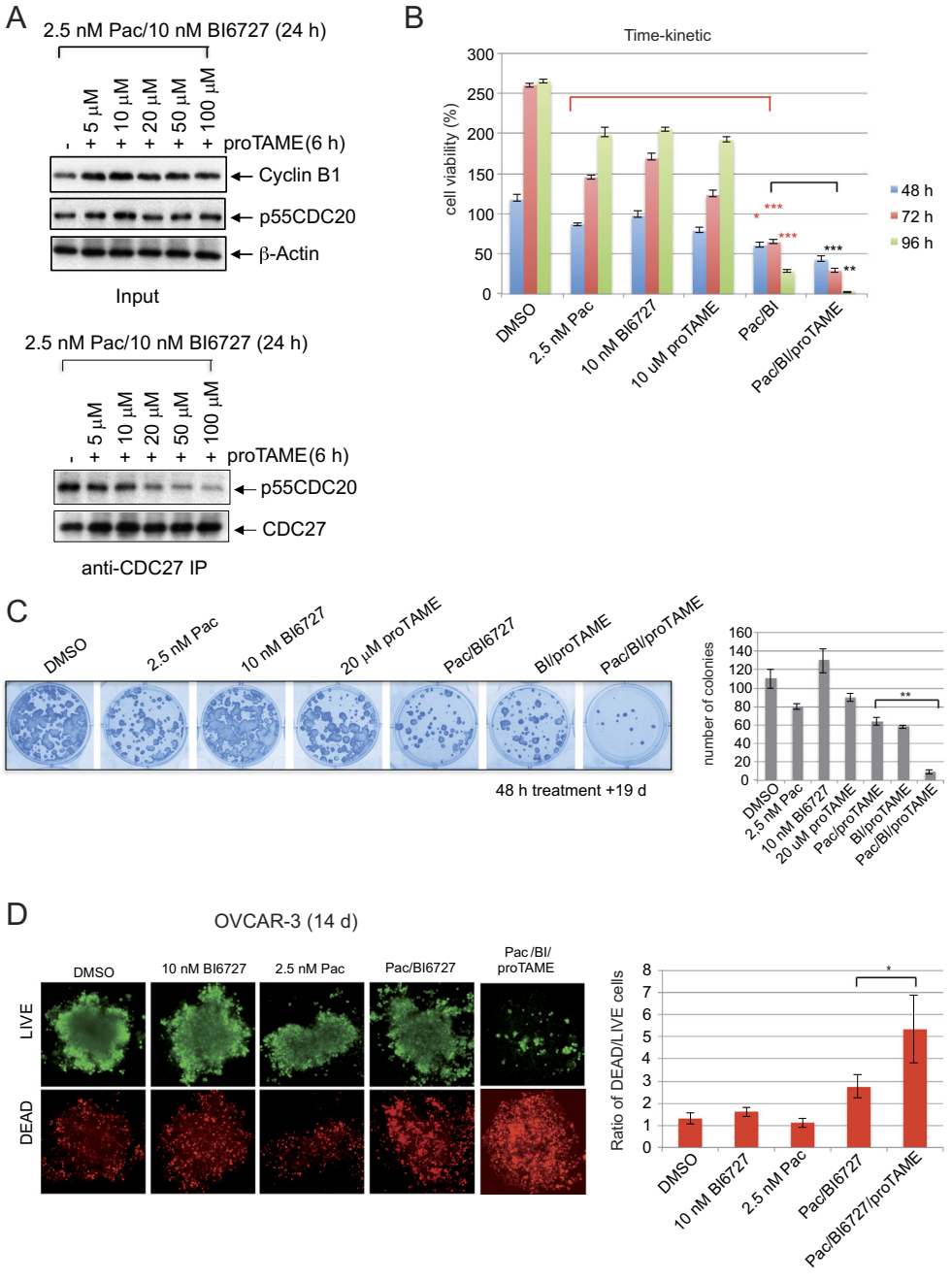

Figure 2. Combinatorial treatment of mitotic OVCAR-3 cells with the APC/C inhibitor proTAME induces a long-lasting inhibition of cell growth. (A) OVCAR-3 cells were treated for 24 hours with paclitaxel and BI6727 followed by a 6-hour treatment with proTAME. Whole cell lysates were used for co-immunoprecipitation experiments with CDC27 antibodies followed by western blotting using antibodies (lower panel) for CDC20 and (upper panel) for Cyclin B1, CDC27, and β-Actin. (B) OVCAR-3 cells were treated for up to 96 hours with 2.5 nM paclitaxel (Pac), 10 nM BI6727, 10 μM proTAME, 2.5 nM Pac/10 nM BI6727, or 2.5 nM Pac/10 nM BI6727/10 μM proTAME for the determination of cell viability (*$P \leq .05$; **$P \leq .01$; ***$P \leq .001$). (C) Coomassie-stained regrown colonies of OVCAR-3 cells treated with 2.5 nM paclitaxel, 10 nM BI6727, 20 μM proTAME, or combinations thereof. The number of colonies was determined after 21 days. Numbers were statistically significant by two-tailed Student's *t* test (**$P \leq .01$). Each bar graph represents the mean value ± SEM ($n=3$). (D) OVCAR-3 cells were grown as 3D culture over 14 days and treated with 10 nM BI6727, 2.5 nM Pac, and/or 20 μM proTAME. Cells were stained using the LIVE/DEAD viability/cytotoxicity kit, and ratios of viable/dead cells were calculated. Measurements were statistically significant by two-tailed Student's *t* test (*$P \leq .05$). Each bar graph represents the mean value ± SEM ($n=3$).

decrease in the viability of mitotic OVCAR-3 cells of treatment with paclitaxel/BI6727/proTAME, which left only 3% of ovarian cancer cells after 96 hours (Figure 2*B*).

In a second long-term experiment, we studied the ability of cells to survive and to form colonies (Figure 2*C*). The experiments revealed that paclitaxel, BI6727, and proTAME acted together to significantly reduce the colony-forming ability (DMSO control 120 colonies; 2.5 nM paclitaxel 78 colonies; 10 nM BI6727 110 colonies; 20 μM proTAME 82 colonies; 2.5 nM paclitaxel/10 nM BI6727 60 colonies, 10 nM BI6727/20 μM proTAME 58 colonies; 2.5 nM paclitaxel/10 nM BI6727/20 μM proTAME 10 colonies) ($P < .01$) (Figure 2*C*).

Recently, a growing body of evidence has indicated that three-dimensional (3D) cell culture systems represent more accurately the actual microenvironment where cells reside in tissues. Therefore, we tested in a third long-term experiment the cell viability in a 3D multicellular model which is widely used as avascular tumor model for metastasis and invasion research. We could demonstrate that the triple combination has the most intense inhibitory effect compared to the combination paclitaxel/BI6727 and compared to the single agents (Figure 2*D*).

Furthermore, we tested the long-term effects in SKOV-3 cells. We observed for all single treatments a weak to moderate inhibitory effect on cell growth over 5 days (Supplementary Figure S4*A*). The triple combination was significantly more efficient to inhibit the growth compared to the treatment with paclitaxel/BI6727 ($P < .001$) (Supplementary Figure S4*A*). Furthermore, the 48-hour treatment of SKOV-3 cells followed by a 10-day observation period showed the most intense inhibition of colony formation using the triple combination compared to double or single treatments (Supplementary Figure S4*B*, upper and lower panel). Together, different long-term analyses revealed that the triple combination is much more efficient in inhibiting viability and colony formation of different ovarian cancer cell lines compared to paclitaxel or the combination paclitaxel/BI6727.

APC/C Inhibitors Increase Apoptosis in Mitotically Arrested Ovarian Cancer Cells

Very low levels of Caspase-3/7 activation in OVCAR-3 cells could be detected after single treatments compared to controls (Figure 3*A*). This activation could be enhanced by incubation with paclitaxel/BI6727 [2.5 nM paclitaxel/20 nM BI6727 activation to 3.5-fold compared with 2.5 nM paclitaxel ($P < .001$)] and even further by the triple treatment [20 nM BI6727/2.5 nM paclitaxel/10 μM proTAME activation to 6.8-fold compared with paclitaxel/BI6727 ($P < .01$)]. The FACS analysis showed a significant increase of the sub G_0/G_1 peak indicating an apoptotic cell population comparing paclitaxel/BI6727 versus paclitaxel/BI6727/ proTAME-treated cells ($P < .05$) (Figure 3*B*). Furthermore, cells were stained with PE Annexin V/7-AAD and analyzed by FACS. We observed a moderate increase of Annexin V–positive cells after an incubation with paclitaxel for 48 hours (2.5 nM, 12%), BI6727 (20 nM, 11%), or proTAME (10 μM, 10%) compared to controls (DMSO, 7%) (Figure 3*C*). The co-incubation of cells for 48 hours with 20 nM BI6727 and paclitaxel induced 13% PE Annexin V/7-AAD–positive cells versus 17% positive cells following 2.5 nM paclitaxel/20 nM BI6727/10 μM proTAME (Figure 3*C*). The examination of apoptosis in SKOV-3 cells based on Caspase-3/7 activation, sub G_0/G_1 peak, and PE Annexin V/7-AAD staining confirmed our observations from OVCAR-3 cells (Figure S5, *A-C*) showing that the triple treatment induces significantly more apoptosis in ovarian cancer cell lines compared to single or double treatments ($P < .01$).

We examined members of the antiapoptotic BCL-2 family, which contribute to the regulation of apoptosis during mitotic arrest [48]. In contrast to the treatment with single agents, the combinatorial treatment (paclitaxel/BI6727) prompted elevated levels of BCL-XL phosphorylation and cleavage of PARP and Caspase-3, respectively, with the highest levels in triple-treated cells (Figure 3*D*, upper panel). Recent studies describe a pathway involving the protein myeloid cell leukemia 1 (MCL-1), an antiapoptotic member of the BCL-2 family, that couples the timing of mitosis to the induction of apoptosis [48]. PLK1 was shown to regulate the stability of FBW7, promoting the degradation of MCL-1 [49]. While the co-treatment with BI6727/paclitaxel decreased the MCL-1 level, the triple treatment led to further degradation of MCL-1 (Figure 3*D*, lower panels). High levels of PLK1, Securin, and phopho-Histone H3 in co-treated cells suggest that the inactivation of antiapoptotic BCL-2 family members (downregulation of MCL-1, phosphorylation of BCL-XL) occurs in mitosis (Figure 3*D*, upper and lower panel). In summary, BI6727, paclitaxel, and proTAME cooperate to activate the mitochondrial pathway, leading to the activation of Caspase-3 (Figure 3, *A* and *D*).

Preventing Mitotic Exit Increases Cellular Death in Mitosis

To assess the fate of cells following drug treatment in more detail, we analyzed SAC activity by monitoring the mitotic exit. OVCAR-3 cells stably transfected with mCherry-H2B were synchronized in the S-phase, released in media with drugs, and followed by time-lapse microscopy (Figure 4*A*). While control cells completed mitosis normally (1.1 ± 0.12 hours), paclitaxel significantly increased mitotic duration (17.5 ± 5.4 hours) (Figure 4, *B* and *C*). The combinatorial treatment (paclitaxel/BI6727) caused a prolonged mitotic arrest (19.0 ± 4.5 hours) (Figure 4, *B* and *C*). Remarkably, the triple treatment significantly shortens the time in mitotic arrest compared to paclitaxel (11.5 ± 3.2 vs. 17.5 ± 5.4 hours) (Figure 4, *B* and *C*). To shed more light on the cell fate induced by different applications, we tracked the outcome of single cells during mitotic arrest and after mitotic exit. Two percent of DMSO-treated cells died during mitotic arrest; 2% could evade mitosis but died in the next interphase (Figure 4*D*). Drug treatment had differential effects on the death in mitosis (paclitaxel, 35%; paclitaxel/BI6727, 45%; paclitaxel/BI6727/proTAME 100%) or death in interphase (paclitaxel, 2%; paclitaxel/BI6727, 10%; paclitaxel/BI6727/ proTAME 0%), showing that the strong mitotic arrest induced by the triple combination is associated with highly frequent death in mitosis (Figure 4*D*). The observations revealed that triple-treated cells have a short resting time in mitosis because they die before they can exit mitosis. While treatment with paclitaxel and paclitaxel/BI6727 increased endoreduplication, only the triple combination blocked endoduplication completely, indicating that an increase in genetic complexity is prevented (Figure 4*E*).

Blocking Mitotic Exit Reduces Chromosome Numbers in Mitotically Arrested Ovarian Cells

The ability to assess chromosome abnormalities based on the analysis of metaphase chromosome spreads can reveal genetic disorders in cells that have survived the drug treatment. The cell line OVCAR-3 is aneuploid human female, with chromosome counts in the sub- to near triploid range [50]. OVCAR-3 cells were treated for 24 hours with single agents (2.5 nM paclitaxel, 20 nM BI6727) followed by 10 μM proTAME for 24 hours and thereafter transferred to compound-free medium for 14 days followed by examination of metaphase spreads of the surviving cells (Figure 5, *A* and *B*). The mean number of chromosomes

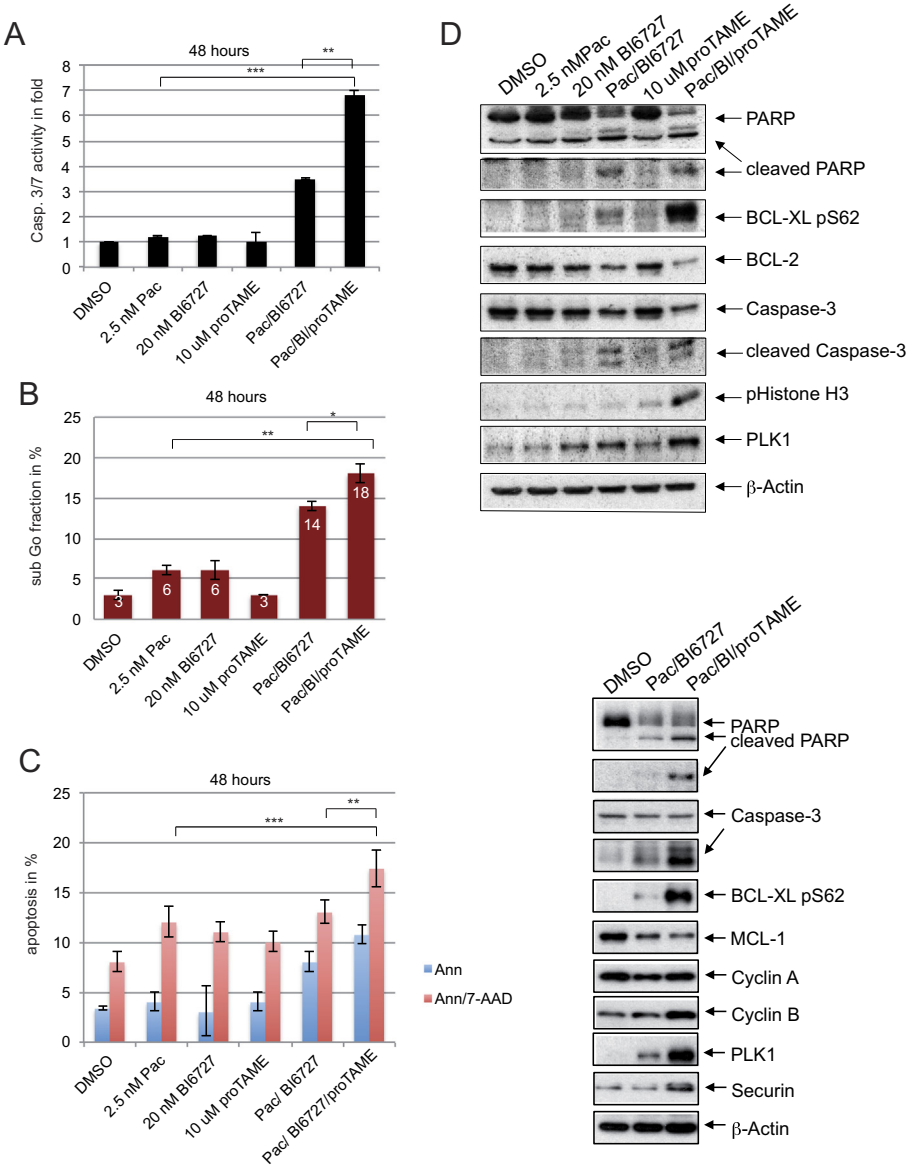

Figure 3. Induction of apoptosis in ovarian cancer cells following drug treatment. (A) OVCAR-3 cells were incubated with 2.5 nM paclitaxel, 20 nM BI6727, 10 μM proTAME, or combinations thereof. Caspase-3/7 activity in whole cell lysates was measured 48 hours posttreatment using the Caspase-Glo 3/7 Assay. Each bar graph represents the mean value ± SEM (n=3). Apoptosis was validated (B) by measuring the sub G_0/G_1 fractions or (C) by PE Annexin V staining. Measurements were statistically significant by two-tailed Student's t test (*$P \leq .05$; **$P \leq .01$, ***$P \leq .001$). Each bar graph represents the mean value ± SEM (n=3). (D ,upper and lower panel) Whole cell lysates of OVCAR-3 cells were analyzed evaluating marker proteins for mitochondrial-mediated apoptosis. Endogenous levels of PARP, cleaved PARP, BCL-XL pS62, BCL-2, Caspase-3, cleaved-Caspase-3, pHistone H3, PLK1, Cyclin B1, MCL-1, Cyclin A, Securin, and β-Actin were determined by immunoblotting.

per cell 63.37 ± 8.75 in the OVCAR-3 population increased in cells that survived the 48-hour treatment with 2.5 nM paclitaxel to 72.76 ± 17.63, with 20 nM BI6727 to 99.86 ± 21.37, and with 2.5 nM paclitaxel/20 nM BI6727 to 121.80 ± 20.08. Cells that survived the 48-hour triple treatment showed very similar chromosome numbers (65.04 ± 7.43) compared to DMSO-treated cells (Figure 5*C*). Chromosome spreading in SKOV-3 cells showed again that cells treated with paclitaxel/BI6727/proTAME had very similar chromosome numbers compared to untreated cells (Supplementary Figure S6, *A-C*), supporting the view that the treatment with proTAME counteracts the chromosomal instability in ovarian cancer cells induced by paclitaxel and/or BI6727.

Evaluation of the Treatment-Associated Toxicity in Normal Primary Mammalian Cells

Next, we evaluated the correlation between drug treatment and growth of primary human cells. Remarkably, the cell growth of fibroblasts was robust in single, double, and triple treatments over 96 hours, suggesting that the toxicity of the agents at least at the concentrations used in our experiments is very low in primary fibroblasts (Supplementary Figure S7).

Blocking Mitotic Exit Inhibits the Growth of Mitotically Arrested Primary, Patient-Derived Ovarian Cancer Cells

To study the physiological relevance of our experiments, we extended our study to a primary ovarian cancer cell culture established

from tumor specimen derived from patients diagnosed with ovarian cancer. For all single agents (paclitaxel >0.1 nM, BI6727> 8 nM, proTAME >10 μM), a dose-dependent decrease in the viability of primary ovarian cancer cells was observed (Figure 6*A*). Within the range of tested concentrations, proTAME exerted the most intense inhibitory effect. Increasing concentrations in the range of 0-100 nM paclitaxel was not sufficient to reduce the growth of primary cells by 50%. In combinatorial approaches including 100 nM BI6727, the

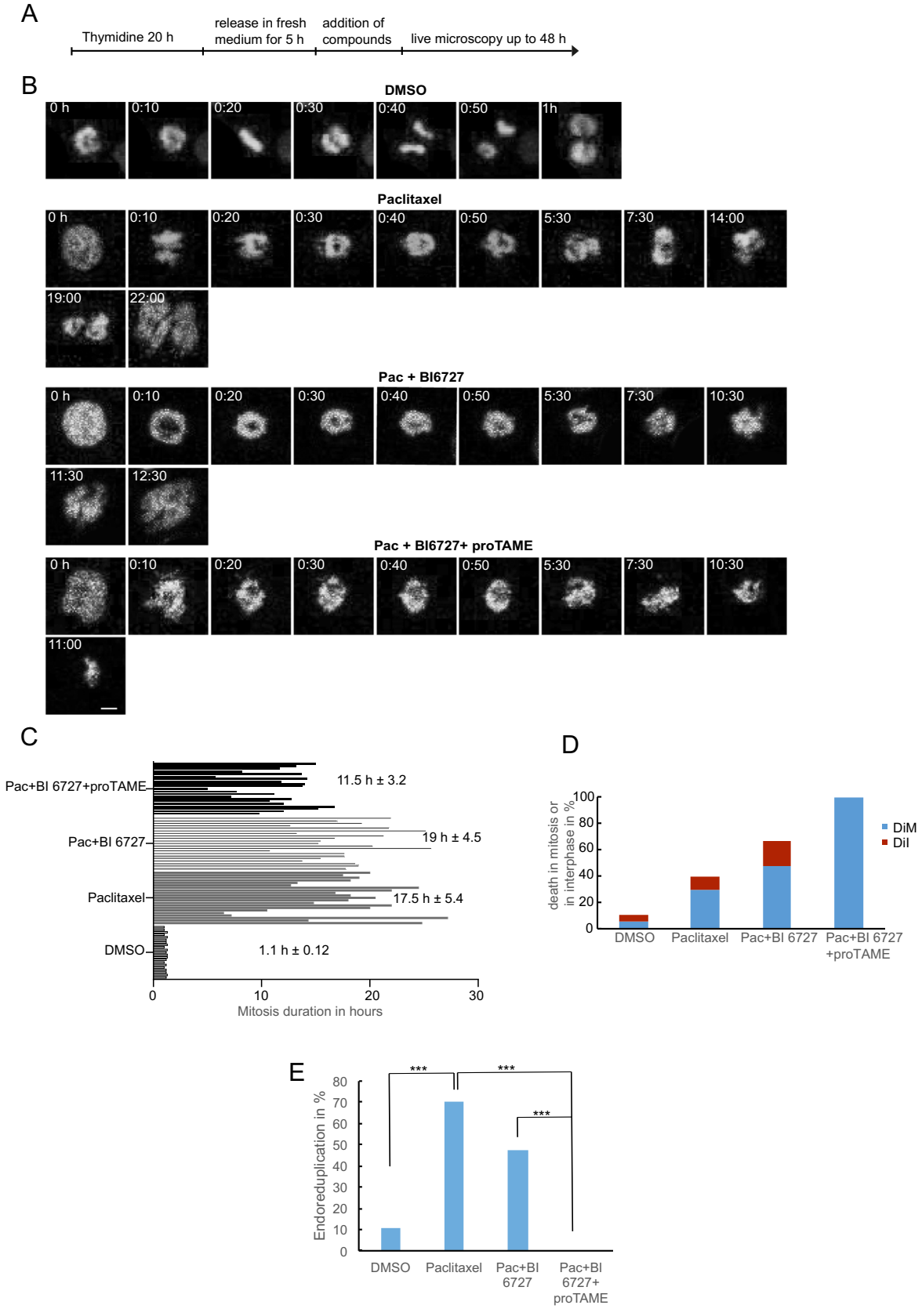

IC_{50} for paclitaxel was determined to be 4 nM; with 100 nM BI6727/15 μM, the IC_{50} for paclitaxel was significantly reduced to 0.7 nM ($P < .001$) (Figure 6*B*).

The addition of proTAME to primary cells treated with the two mitotic inhibitors paclitaxel and BI6727 in long-term experiments (6 days) augmented the growth inhibition significantly ($P < .001$) (Figure 6*C*). The analysis of the Caspase 3/7 activity supported the observation from long-term cultures that the triple treatment exerts the most intense apoptosis compared to the double or single treatments ($P < .05$) (Figure 6*D*). Results with 3D cultures revealed a significant increase of dead cells by the combinatorial treatment including proTAME compared to single and double treatments ($P < .05$) (Figure 6*E*).

Furthermore, we analyzed multiple additional samples from recurrent ovarian cancer disease (Figure S8). The triple treatment showed again a significant reduction of cell viability, 3D-colony formation in short- and long-term experiments, and apoptosis measurements by Annexin staining (Figure S8, *A-E*). Although the triple combination induced the most pronounced growth inhibitory effects, the IC_{50} for paclitaxel treating primary tumor samples was lower compared to samples derived from recurrent disease (Figure 6, Supplementary Figure S8, *A-E*). Our observations support the clinical relevance of this combinatorial approach in primary ovarian cancer.

Discussion

Despite two trials [International Collaborative Ovarian Neoplasm (ICON) 1 and ACTION] that were conducted to address the uncertain survival benefit of immediate adjuvant chemotherapy in early-stage disease [51,52], there is no clear consensus for systemic treatment of early stage patients yet. Since the choice of the optimal adjuvant chemotherapy regimen and the duration of treatment in early-stage EOC are subjects of continuing debate, additional markers for an improved stratification of early-stage EOC patients are urgently needed for a more precise definition of optimal chemotherapeutic regimens. Here, we could demonstrate that ovarian cancer patients in stages I and II with high PLK1 expression (62 months) had a shorter progression-free survival compared to patients with low PLK1 expression (76 months), suggesting that PLK1 is a novel marker for the stratification of early-stage ovarian cancer patients to maximize therapeutic efforts. In addition, PLK1 is a promising target in ovarian cancer cells for the induction of synthetic lethality [53] and in clinical trials for ovarian cancer patients [39].

While the microtubule-targeting drug paclitaxel has impressive clinical efficacy in ovarian tumors and other types of cancer, the exact mechanisms of how this drug yields patient benefit and why chemoresistance is still a major issue for many paclitaxel-treated ovarian cancer patients remain to be elucidated [54]. This is in part because construction of the microtubule apparatus that constitutes the mitotic spindle responsible for chromosome segregation and cell division encompasses a plethora of regulatory events. Perturbating the superstructure of the spindle apparatus activates the SAC, leading to a prolonged mitotic arrest [55]. After a prolonged mitotic arrest, cells either die in mitosis or exit with still incomplete cell division and return to interphase, which is called slippage [9–11]. In response to paclitaxel, failure to undergo death in mitosis and/or failure to efficiently engage postmitotic responses can lead to proliferation of cells with highly abnormal genomes [56]. In this study, we used a "two-punch strategy" to intensify the mitotic arrest and block mitotic exit, aiming to increase the percentage of cells that undergo death in mitosis, which could lower the number of surviving aneuploid cells. Treatment with paclitaxel and BI6727 induced a strong mitotic arrest in ovarian cancer cells (Figure 4, Supplementary Figure S3). Experiments focusing on cell growth, cell cycle distribution, and apoptosis revealed that a pretreatment with paclitaxel and BI6727 followed by proTAME (triple combination) is very efficient to induce cells death (Figures 3 and 6, Supplementary Figure S5), i.e., combining BI6727 and proTAME is not only a promising strategy to reduce the inhibitory concentration of paclitaxel efficiently (Supplementary Figures S1 and S2), but this "two-punch strategy" increases also the percentage of mitotic cell death significantly as demonstrated in our time-lapse experiments (Figure 4). Increased cell death could be further substantiated in long-term and in 3D cultures (Figure 2, Supplementary Figure S4). Based on our knowledge about apoptotic signaling during an extended mitotic arrest induced by agents that deregulate microtubule dynamics, two approaches to increase the efficacy of microtubule-targeting drugs like paclitaxel are 1) prolonging mitotic arrest and 2) speeding up the decay/degradation of the apoptotic timer MCL-1, i.e., to shift the balance from cell survival to apoptosis, the rate of Cyclin B1 degradation needs to be slowed and the rate of MCL-1 degradation must be increased. In our study, we could show that proTAME prevents binding of CDC20 to CDC27, preventing efficient activation of the APC/C in ovarian cancer cells. According to this strategy, we could stabilize the pool of mitotic Cyclin B1 (Figures 2*A* and 3*D*), which extends the mitotic arrest, giving cells sufficient time to activate the apoptotic machinery.

Furthermore, antiapoptotic BCl-XL and MCL-1 have been shown to be important mitotic survival factors, and cell showing an elevated BCL-XL level are demonstrated to be less responsive to taxane-based therapy [57]. In our study, we showed that the triple combination could achieve two very important results: 1) to increase the proapoptotic phosphorylation of BCL-XL (pS62) and 2) to reduce the levels of MCL-1 based on an FBW7/PLK1-based mechanism. By acting on BCL-XL and MCL-1, the arrested cells lose the prosurvival signaling rapidly (within 16 hours in our experiments), which quickly triggers apoptosis and explains the reduced time in mitotic arrest and quick death in mitosis according to our time-lapse experiment.

The clinical relevance of our data was shown in experiments using primary ovarian cancer cells from different patients (Figure 6, Supplementary Figure S8). While the triple combination induced

Figure 4. Combinatorial treatment of mitotic OVCAR-3 cells with proTAME promotes death in mitosis and blocks endoreduplication. (A) Treatment schedule for time-lapse microscopy. Cells were first incubated with 2 mM thymidine to arrest them in the S-phase. After releasing the cells in fresh medium for 5 hours, drugs were added to cells and time-lapse microscopy was started up to 48 hours. (B) Representative time-lapse of OVCAR-3 cells expressing mcherry-H2B treated as in (A) with 1 nM paclitaxel, 1 nM paclitaxel/10 nM BI6727, or 1 nM paclitaxel/10 nM BI6727/10 μM proTAME (from $t = 0$ hour to $t = 48$ hours). Scale bar: 10 μm. (C) Duration of mitosis in OVCAR-3 cells treated with 1 nM paclitaxel, 1 nM paclitaxel/10 nM BI6727, or 1 nM paclitaxel/10 nM BI6727/10 μM proTAME was assessed by time-lapse microscopy. Mitotic duration of each cell in the different treatment groups ($n = 40$) is quantitated in the bar graph. (D) Rate of cells exhibiting death in mitosis (DiM) or death in interphase (DiI) observed in the different treatment groups in percentage. (E) Endoreduplication rate observed in the different treatment groups in percentage (***$P \leq .001$).

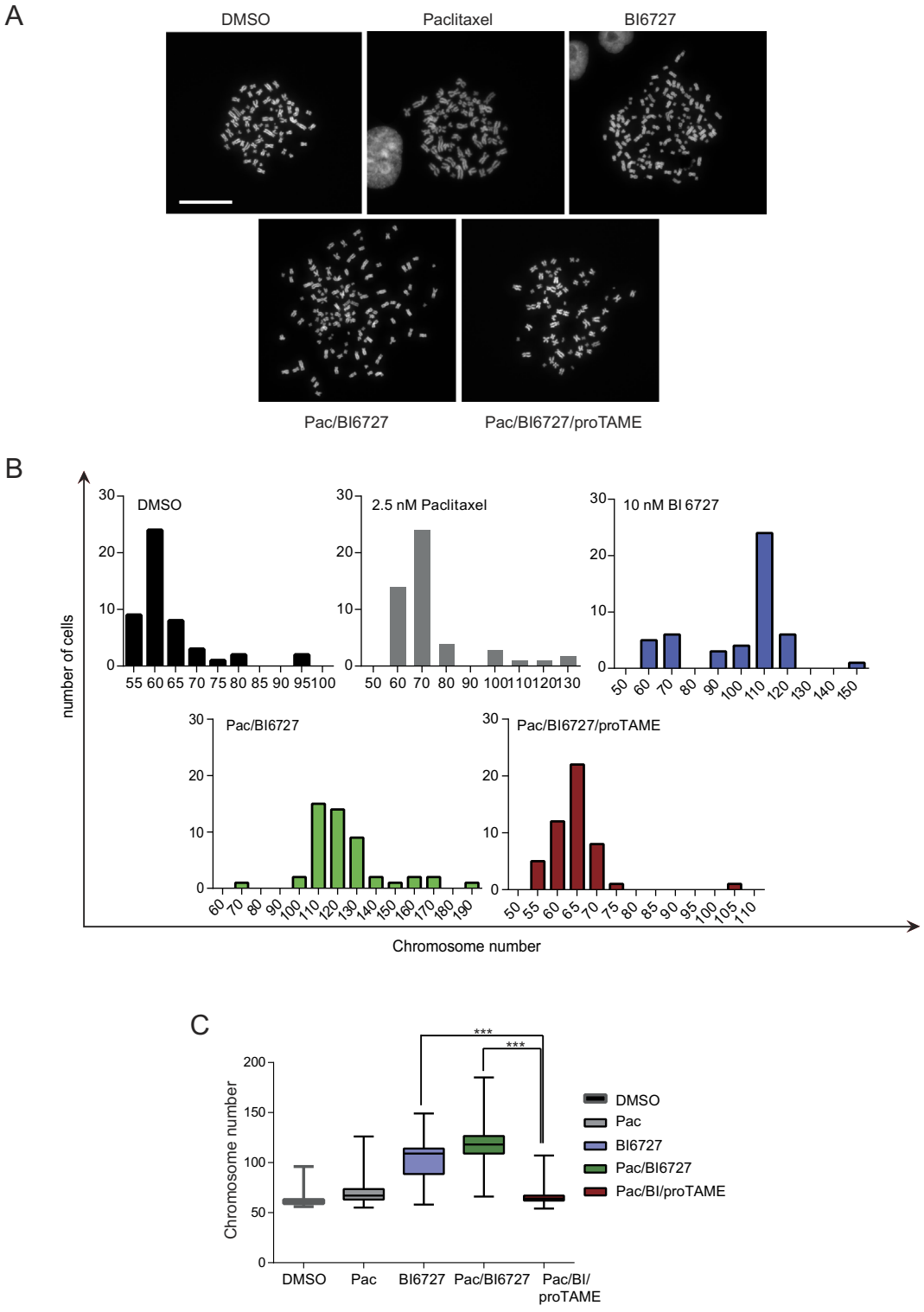

Figure 5. Analysis of chromosomal aberrations in drug-treated ovarian cancer cells. (A) Following the incubation with single (2.5 nM paclitaxel, 10 nM BI6727, 10 μM proTAME), double, or triple agents for 48 hours and subsequent release into fresh medium for 14 days, metaphase spreads of treated OVCAR-3 cells were prepared, and the chromosomes were stained with Hoechst. Scale bar: 20 μm (B) The histogram plotting of the distribution of chromosome numbers at day 14 is shown. (C) Quantification of the number of chromosomes in 500 OVCAR-3 cells incubated in the presence of different agents for 48 hours. Measurements were statistically significant by two-tailed Student's *t* test (***$P < .001$). Each bar graph represents the mean value ± SEM ($n=3$).

pronounced apoptosis in primary ovarian cancer cells, the induction of apoptosis was very low in primary normal human cells, suggesting a favorable therapeutic window for this combinatorial approach (Supplementary Figure S7).

Unequal chromosome distribution during cell division as a mechanism that contributes to chromosomal instability (CIN) is a feature associated with many types of cancer. CIN results from errors in DNA replication, DNA repair, or chromosomal mis-segregation

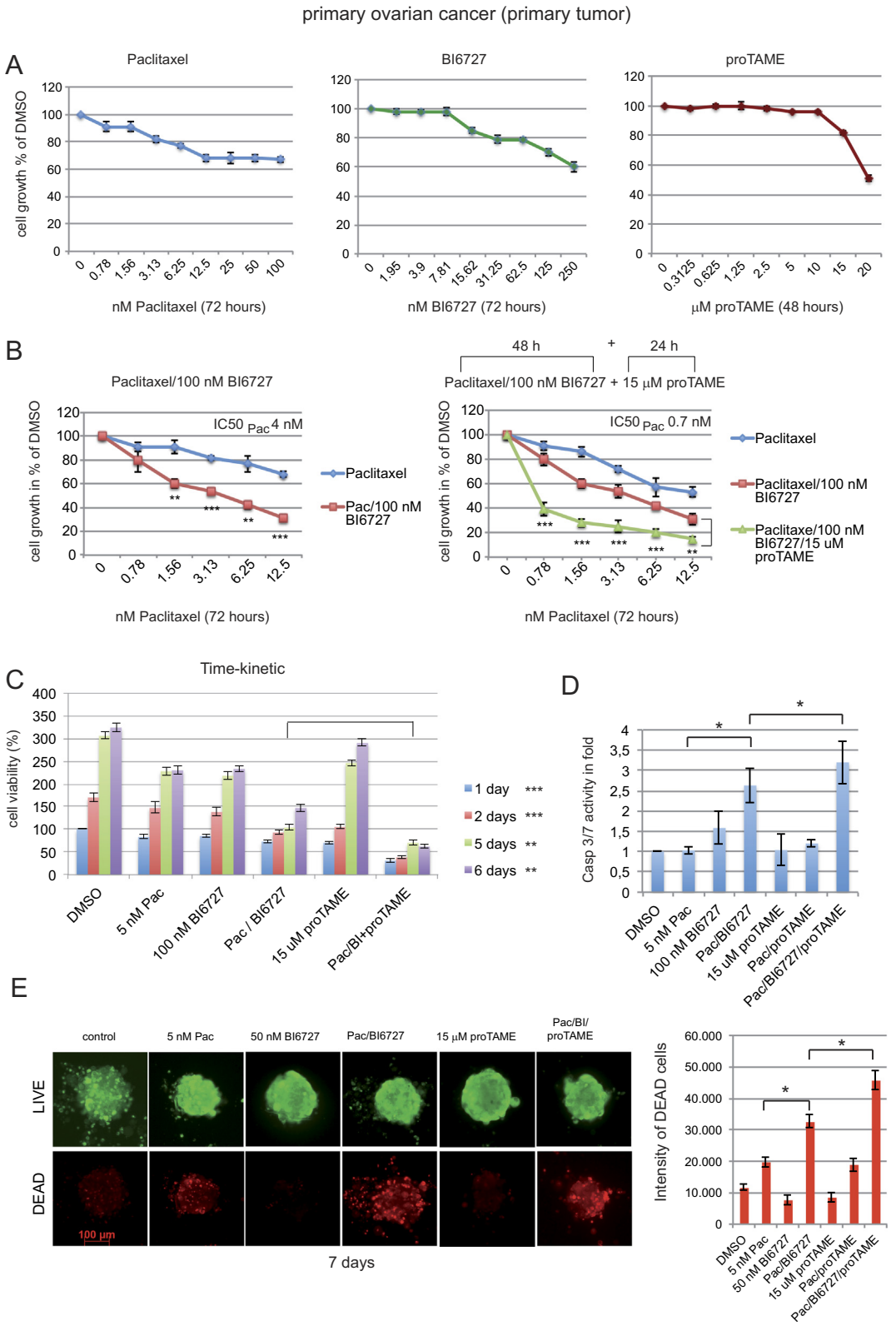

Figure 6. Blocking mitotic exit sensitizes ovarian cancer patient-derived primary cells to paclitaxel. (A) Primary tumor cells were treated with increasing concentrations of paclitaxel, BI6727, or proTAME or combinations. (B) The cell viability was determined after 72 hours or (C) over a period of 6 days using the Cell Titer-Blue Cell Viability Assay. (D) After treatment for 48 hours Caspase 3/7 activity was measured using the Caspase-Glo 3/7 assay. (E) 3D cultures grown out of primary tumor cells were treated (5 nM paclitaxel, 50 nM BI6727, 15 μM proTAME, or combinations thereof), cells were stained, and fluorescence intensities of dead cells were determined. Measurements were statistically significant by two-tailed Student's *t* test (*$P \leq .05$). Each bar graph represents the mean value ± SEM ($n=3$).

[58]. CIN is of particular interest because it is associated with aggressive tumors, the acquisition of drug resistance, and poor patient prognosis [59–62]. Multiple investigations described genome instability in ovarian cancer [63–65], which is characterized by gene copy number variations, rearranged genomes, structural variants, and single nucleotide variants. The treatment with paclitaxel and BI6727 increased chromosome numbers in ovarian cancer cells significantly (Figure 5, Supplementary Figure S6). This result correlates with our previous observations showing that BI6727 induces slippage associated with mis-segregation of chromosomes [66]. Only the triple treatment induced a high percentage of cells blocked in mitosis, thereby preventing an increase in chromosome numbers and preventing endoreduplication (Figures 4 and 5, Supplementary Figure S6). Endoreplication can contribute to genome instability [67]. Recent work revealed that cancer cells use endoreplication as a path to drug resistance: Several cancer cell lines treated with growth-suppressing drugs enter endoreplication cycles [68,69]. Severe reduction of this process in triple-treated cells could reduce the oncogenic potential and chemoresistance in ovarian cancer cells. Together, by using the APC/C inhibitor proTAME for the treatment of mitotically arrested cells, we could present a tumor cells-suppressing strategy that is characterized by slippage inhibition and significant downregulation of chromosomal instability resulting in minimized long-term growth of ovarian cells.

Conclusions

Here, for the first time, our Kaplan-Meier analysis demonstrated the prognostic role of PLK1 expression in a cohort of 263 early-stage (I/II) ovarian cancer patients. We considered PLK1 as an ovarian cancer target and applied a combinatorial strategy using paclitaxel and a small molecule inhibitor of PLK1 to induce a strong mitotic arrest in ovarian cancer cells followed by an inhibition of the anaphase-promoting complex. By preventing the mitotic exit of ovarian cancer cells, this "two-punch strategy" reduces endoreduplication and strongly increases apoptosis. We revealed that this drug combination reduces mitotic slippage of paclitaxel-treated cells and reduces chromosomal instability, which is often associated with aggressive tumors and the acquisition of drug resistance. Thus, the "two punch strategy" might open novel avenues for the development of paclitaxel-based therapies of ovarian cancer patients.

Supplementary data to this article can be found online at https://doi.org/10.1016/j.neo.2019.01.007.

Acknowledgements

This work was supported by grants from the Messer Stiftung (Germany), Research Support Foundation (Switzerland), Deutsche Krebshilfe (Germany), BANNS Stiftung (Germany), and DKTK (Germany).

References

[1] Karnezis AN, Cho KR, Gilks CB, Pearce CL, and Huntsman DG (2017). The disparate origins of ovarian cancers: pathogenesis and prevention strategies. *Nat Rev Cancer* **17**, 65–74.

[2] Yang Q, Yang Y, Zhou N, Tang K, Lau WB, Lau B, Wang W, Xu L, Yang Z, and Huang S, et al (2018). Epigenetics in ovarian cancer: premise, properties, and perspectives. *Mol Cancer* **17**, 109.

[3] Montero A, Fossella F, Hortobagyi G, and Valero V (2005). Docetaxel for treatment of solid tumours: a systematic review of clinical data. *Lancet Oncol* **6**, 229–239.

[4] Bolis G, Scarfone G, Raspagliesi F, Mangili G, Danese S, Scollo P, Lo Russo D, Villa A, Aimone PD, and Scambia G (2010). Paclitaxel/carboplatin versus topotecan/paclitaxel/carboplatin in patients with FIGO suboptimally resected stage III-IV epithelial ovarian cancer a multicenter, randomized study. *Eur J Cancer* **46**, 2905–2912.

[5] du Bois A, Luck HJ, Meier W, Adams HP, Mobus V, Costa S, Bauknecht T, Richter B, Warm M, and Schroder W, et al (2003). A randomized clinical trial of cisplatin/paclitaxel versus carboplatin/paclitaxel as first-line treatment of ovarian cancer. *J Natl Cancer Inst* **95**, 1320–1329.

[6] Ozols RF, Bundy BN, Greer BE, Fowler JM, Clarke-Pearson D, Burger RA, Mannel RS, DeGeest K, Hartenbach EM, and Baergen R, et al (2003). Phase III trial of carboplatin and paclitaxel compared with cisplatin and paclitaxel in patients with optimally resected stage III ovarian cancer: a Gynecologic Oncology Group study. *J Clin Oncol* **21**, 3194–3200.

[7] Vasey PA, Jayson GC, Gordon A, Gabra H, Coleman R, Atkinson R, Parkin D, Paul J, Hay A, and Kaye SB, et al (2004). Phase III randomized trial of docetaxel-carboplatin versus paclitaxel-carboplatin as first-line chemotherapy for ovarian carcinoma. *J Natl Cancer Inst* **96**, 1682–1691.

[8] Harter P, Sehouli J, Reuss A, Hasenburg A, Scambia G, Cibula D, Mahner S, Vergote I, Reinthaller A, and Burges A, et al (2011). Prospective validation study of a predictive score for operability of recurrent ovarian cancer: the Multicenter Intergroup Study DESKTOP II. A project of the AGO Kommission OVAR, AGO Study Group, NOGGO, AGO-Austria, and MITO. *Int J Gynecol Cancer* **21**, 289–295.

[9] Wimberger P, Roth C, Pantel K, Kasimir-Bauer S, Kimmig R, and Schwarzenbach H (2011). Impact of platinum-based chemotherapy on circulating nucleic acid levels, protease activities in blood and disseminated tumor cells in bone marrow of ovarian cancer patients. *Int J Cancer* **128**, 2572–2580.

[10] Brito DA, Yang Z, and Rieder CL (2008). Microtubules do not promote mitotic slippage when the spindle assembly checkpoint cannot be satisfied. *J Cell Biol* **182**, 623–629.

[11] Gascoigne KE and Taylor SS (2008). Cancer cells display profound intra- and interline variation following prolonged exposure to antimitotic drugs. *Cancer Cell* **14**, 111–122.

[12] Shi J, Orth JD, and Mitchison T (2008). Cell type variation in responses to antimitotic drugs that target microtubules and kinesin-5. *Cancer Res* **68**, 3269–3276.

[13] Rowinsky EK, Eisenhauer EA, Chaudhry V, Arbuck SG, and Donehower RC (1993). Clinical toxicities encountered with paclitaxel (Taxol). *Semin Oncol* **20**, 1–15.

[14] Waters JC, Mitchison TJ, Rieder CL, and Salmon ED (1996). The kinetochore microtubule minus-end disassembly associated with poleward flux produces a force that can do work. *Mol Biol Cell* **7**, 1547–1558.

[15] Foley EA and Kapoor TM (2013). Microtubule attachment and spindle assembly checkpoint signalling at the kinetochore. *Nat Rev Mol Cell Biol* **14**, 25–37.

[16] Kops GJ, Weaver BA, and Cleveland DW (2005). On the road to cancer: aneuploidy and the mitotic checkpoint. *Nat Rev Cancer* **5**, 773–785.

[17] Lara-Gonzalez P, Westhorpe FG, and Taylor SS (2012). The spindle assembly checkpoint. *Curr Biol* **22**, R966-980.

[18] Peters JM (2006). The anaphase promoting complex/cyclosome: a machine designed to destroy. *Nat Rev Mol Cell Biol* **7**, 644–656.

[19] Sackton KL, Dimova N, Zeng X, Tian W, Zhang M, Sackton TB, Meaders J, Pfaff KL, Sigoillot F, and Yu H, et al (2014). Synergistic blockade of mitotic exit by two chemical inhibitors of the APC/C. *Nature* **514**, 646–649.

[20] Zeng X, Sigoillot F, Gaur S, Choi S, Pfaff KL, Oh DC, Hathaway N, Dimova N, Cuny GD, and King RW (2010). Pharmacologic inhibition of the anaphase-promoting complex induces a spindle checkpoint-dependent mitotic arrest in the absence of spindle damage. *Cancer Cell* **18**, 382–395.

[21] Strebhardt K and Ullrich A (2006). Targeting polo-like kinase 1 for cancer therapy. *Nat Rev Cancer* **6**, 321–330.

[22] Zitouni S, Nabais C, Jana SC, Guerrero A, and Bettencourt-Dias M (2014). Polo-like kinases: structural variations lead to multiple functions. *Nat Rev Mol Cell Biol* **15**, 433–452.

[23] Lee KS and Erikson RL (1997). Plk is a functional homolog of Saccharomyces cerevisiae Cdc5, and elevated Plk activity induces multiple septation structures. *Mol Cell Biol* **17**, 3408–3417.

[24] Wolf G, Elez R, Doermer A, Holtrich U, Ackermann H, Stutte HJ, Altmannsberger HM, Rubsamen-Waigmann H, and Strebhardt K (1997). Prognostic significance of polo-like kinase (PLK) expression in non-small cell lung cancer. *Oncogene* **14**, 543–549.

[25] Wolf G, Hildenbrand R, Schwar C, Grobholz R, Kaufmann M, Stutte HJ, Strebhardt K, and Bleyl U (2000). Polo-like kinase: a novel marker of proliferation: correlation with estrogen-receptor expression in human breast cancer. *Pathol Res Pract* **196**, 753–759.

[26] Knecht R, Oberhauser C, and Strebhardt K (2000). PLK (polo-like kinase), a new prognostic marker for oropharyngeal carcinomas. *Int J Cancer* **89**, 535–536.

[27] Strebhardt K, Kneisel L, Linhart C, Bernd A, and Kaufmann R (2000). Prognostic value of pololike kinase expression in melanomas. *JAMA* **283**, 479–480.
[28] Liu X and Erikson RL (2003). Polo-like kinase 1 in the life and death of cancer cells. *Cell Cycle* **2**, 424–425.
[29] Park JE, Li L, Park J, Knecht R, Strebhardt K, Yuspa SH, and Lee KS (2009). Direct quantification of polo-like kinase 1 activity in cells and tissues using a highly sensitive and specific ELISA assay. *Proc Natl Acad Sci U S A* **106**, 1725–1730.
[30] Weichert W, Denkert C, Schmidt M, Gekeler V, Wolf G, Kobel M, Dietel M, and Hauptmann S (2004). Polo-like kinase isoform expression is a prognostic factor in ovarian carcinoma. *Br J Cancer* **90**, 815–821.
[31] Takahashi T, Sano B, Nagata T, Kato H, Sugiyama Y, Kunieda K, Kimura M, Okano Y, and Saji S (2003). Polo-like kinase 1 (PLK1) is overexpressed in primary colorectal cancers. *Cancer Sci* **94**, 148–152.
[32] Yamada S, Ohira M, Horie H, Ando K, Takayasu H, Suzuki Y, Sugano S, Hirata T, Goto T, and Matsunaga T, et al (2004). Expression profiling and differential screening between hepatoblastomas and the corresponding normal livers: identification of high expression of the PLK1 oncogene as a poor-prognostic indicator of hepatoblastomas. *Oncogene* **23**, 5901–5911.
[33] Rodel F, Keppner S, Capalbo G, Bashary R, Kaufmann M, Rodel C, Strebhardt K, and Spankuch B (2010). Polo-like kinase 1 as predictive marker and therapeutic target for radiotherapy in rectal cancer. *Am J Pathol* **177**, 918–929.
[34] Spankuch-Schmitt B, Wolf G, Solbach C, Loibl S, Knecht R, Stegmuller M, von Minckwitz G, Kaufmann M, and Strebhardt K (2002). Downregulation of human polo-like kinase activity by antisense oligonucleotides induces growth inhibition in cancer cells. *Oncogene* **21**, 3162–3171.
[35] Spankuch B, Heim S, Kurunci-Csacsko E, Lindenau C, Yuan J, Kaufmann M, and Strebhardt K (2006). Down-regulation of Polo-like kinase 1 elevates drug sensitivity of breast cancer cells in vitro and in vivo. *Cancer Res* **66**, 5836–5846.
[36] Spankuch B, Matthess Y, Knecht R, Zimmer B, Kaufmann M, and Strebhardt K (2004). Cancer inhibition in nude mice after systemic application of U6 promoter-driven short hairpin RNAs against PLK1. *J Natl Cancer Inst* **96**, 862–872.
[37] Liu X and Erikson RL (2003). Polo-like kinase (Plk)1 depletion induces apoptosis in cancer cells. *Proc Natl Acad Sci U S A* **100**, 5789–5794.
[38] Takai N, Miyazaki T, Fujisawa K, Nasu K, Hamanaka R, and Miyakawa I (2001). Expression of polo-like kinase in ovarian cancer is associated with histological grade and clinical stage. *Cancer Lett* **164**, 41–49.
[39] Pujade-Lauraine E, Selle F, Weber B, Ray-Coquard IL, Vergote I, Sufliarsky J, Del Campo JM, Lortholary A, Lesoin A, and Follana P, et al (2016). Volasertib versus chemotherapy in platinum-resistant or -refractory ovarian cancer: a randomized phase II Groupe des Investigateurs Nationaux pour l'Etude des Cancers de l'Ovaire Study. *J Clin Oncol* **34**, 706–713.
[40] Rieder CL and Maiato H (2004). Stuck in division or passing through: what happens when cells cannot satisfy the spindle assembly checkpoint. *Dev Cell* **7**, 637–651.
[41] Yamada HY and Gorbsky GJ (2006). Spindle checkpoint function and cellular sensitivity to antimitotic drugs. *Mol Cancer Ther* **5**, 2963–2969.
[42] Huang HC, Shi J, Orth JD, and Mitchison TJ (2009). Evidence that mitotic exit is a better cancer therapeutic target than spindle assembly. *Cancer Cell* **16**, 347–358.
[43] McShane LM, Altman DG, Sauerbrei W, Taube SE, Gion M, Clark GM, and Statistics Subcommittee of the NCIEWGoCD (2005). REporting recommendations for tumor MARKer prognostic studies (REMARK). *Nat Clin Pract Urol* **2**, 416–422.
[44] Ince TA, Sousa AD, Jones MA, Harrell JC, Agoston ES, Krohn M, Selfors LM, Liu W, Chen K, and Yong M, et al (2015). Characterization of twenty-five ovarian tumour cell lines that phenocopy primary tumours. *Nat Commun* **6**, 7419.
[45] Raab M, Kappel S, Kramer A, Sanhaji M, Matthess Y, Kurunci-Csacsko E, Calzada-Wack J, Rathkolb B, Rozman J, and Adler T, et al (2011). Toxicity modelling of Plk1-targeted therapies in genetically engineered mice and cultured primary mammalian cells. *Nat Commun* **2**, 395.
[46] Helmke C, Raab M, Rodel F, Matthess Y, Oellerich T, Mandal R, Sanhaji M, Urlaub H, Rodel C, and Becker S, et al (2016). Ligand stimulation of CD95 induces activation of Plk3 followed by phosphorylation of caspase-8. *Cell Res* **26**, 914–934.
[47] Rudolph D, Steegmaier M, Hoffmann M, Grauert M, Baum A, Quant J, Haslinger C, Garin-Chesa P, and Adolf GR (2009). BI 6727, a Polo-like kinase inhibitor with improved pharmacokinetic profile and broad antitumor activity. *Clin Cancer Res* **15**, 3094–3102.
[48] Wertz IE, Kusam S, Lam C, Okamoto T, Sandoval W, Anderson DJ, Helgason E, Ernst JA, Eby M, and Liu J, et al (2011). Sensitivity to antitubulin chemotherapeutics is regulated by MCL1 and FBW7. *Nature* **471**, 110–114.
[49] Xiao D, Yue M, Su H, Ren P, Jiang J, Li F, Hu Y, Du H, Liu H, and Qing G (2016). Polo-like kinase-1 regulates Myc stabilization and activates a feedforward circuit promoting tumor cell survival. *Mol Cell* **64**, 493–506.
[50] Hamilton TC, Young RC, McKoy WM, Grotzinger KR, Green JA, Chu EW, Whang-Peng J, Rogan AM, Green WR, and Ozols RF (1983). Characterization of a human ovarian carcinoma cell line (NIH:OVCAR-3) with androgen and estrogen receptors. *Cancer Res* **43**, 5379–5389.
[51] Colombo N, Guthrie D, Chiari S, Parmar M, Qian W, Swart AM, Torri V, Williams C, Lissoni A, and Bonazzi C, et al (2003). International Collaborative Ovarian Neoplasm trial 1: a randomized trial of adjuvant chemotherapy in women with early-stage ovarian cancer. *J Natl Cancer Inst* **95**, 125–132.
[52] Trimbos JB, Vergote I, Bolis G, Vermorken JB, Mangioni C, Madronal C, Franchi M, Tateo S, Zanetta G, and Scarfone G, et al (2003). Impact of adjuvant chemotherapy and surgical staging in early-stage ovarian carcinoma: European Organisation for Research and Treatment of Cancer-Adjuvant ChemoTherapy in Ovarian Neoplasm trial. *J Natl Cancer Inst* **95**, 113–125.
[53] Noack S, Raab M, Matthess Y, Sanhaji M, Kramer A, Gyorffy B, Kaderali L, El-Balat A, Becker S, and Strebhardt K (2018). Synthetic lethality in CCNE1-amplified high grade serous ovarian cancer through combined inhibition of Polo-like kinase 1 and microtubule dynamics. *Oncotarget* **9**, 25842–25859.
[54] Weaver BA (2014). How Taxol/paclitaxel kills cancer cells. *Mol Biol Cell* **25**, 2677–2681.
[55] Musacchio A and Salmon ED (2007). The spindle-assembly checkpoint in space and time. *Nat Rev Mol Cell Biol* **8**, 379–393.
[56] Fujiwara T, Bandi M, Nitta M, Ivanova EV, Bronson RT, and Pellman D (2005). Cytokinesis failure generating tetraploids promotes tumorigenesis in p53-null cells. *Nature* **437**, 1043–1047.
[57] Bennett A, Sloss O, Topham C, Nelson L, Tighe A, and Taylor SS (2016). Inhibition of Bcl-xL sensitizes cells to mitotic blockers, but not mitotic drivers. *Open Biol* **6**.
[58] Thompson SL, Bakhoum SF, and Compton DA (2010). Mechanisms of chromosomal instability. *Curr Biol* **20**, R285-295.
[59] Domingues PH, Nanduri LSY, Seget K, Venkateswaran SV, Agorku D, Vigano C, von Schubert C, Nigg EA, Swanton C, and Sotillo R, et al (2017). Cellular prion protein PrPC and ecto-5'-nucleotidase are markers of the cellular stress response to aneuploidy. *Cancer Res* **77**, 2914–2926.
[60] Swanton C, Nicke B, Schuett M, Eklund AC, Ng C, Li Q, Hardcastle T, Lee A, Roy R, and East P, et al (2009). Chromosomal instability determines taxane response. *Proc Natl Acad Sci U S A* **106**, 8671–8676.
[61] Duesberg P, Stindl R, and Hehlmann R (2001). Origin of multidrug resistance in cells with and without multidrug resistance genes: chromosome reassortments catalyzed by aneuploidy. *Proc Natl Acad Sci U S A* **98**, 11283–11288.
[62] Duesberg P, Stindl R, and Hehlmann R (2000). Explaining the high mutation rates of cancer cells to drug and multidrug resistance by chromosome reassortments that are catalyzed by aneuploidy. *Proc Natl Acad Sci U S A* **97**, 14295–14300.
[63] Baumbusch LO, Helland A, Wang Y, Liestol K, Schaner ME, Holm R, Etemadmoghadam D, Alsop K, Brown P, and Australian Ovarian Cancer Study G, et al (2013). High levels of genomic aberrations in serous ovarian cancers are associated with better survival. *PLoS One* **8**e54356.
[64] Bayani J, Paderova J, Murphy J, Rosen B, Zielenska M, and Squire JA (2008). Distinct patterns of structural and numerical chromosomal instability characterize sporadic ovarian cancer. *Neoplasia* **10**, 1057–1065.
[65] Cooke SL, Ng CK, Melnyk N, Garcia MJ, Hardcastle T, Temple J, Langdon S, Huntsman D, and Brenton JD (2010). Genomic analysis of genetic heterogeneity and evolution in high-grade serous ovarian carcinoma. *Oncogene* **29**, 4905–4913.
[66] Raab M, Kramer A, Hehlgans S, Sanhaji M, Kurunci-Csacsko E, Dotsch C, Bug G, Ottmann O, Becker S, and Pachl F, et al (2015). Mitotic arrest and slippage induced by pharmacological inhibition of Polo-like kinase 1. *Mol Oncol* **9**, 140–154.
[67] Fox DT and Duronio RJ (2013). Endoreplication and polyploidy: insights into development and disease. *Development* **140**, 3–12.
[68] Shen H, Moran DM, and Maki CG (2008). Transient nutlin-3a treatment promotes endoreduplication and the generation of therapy-resistant tetraploid cells. *Cancer Res* **68**, 8260–8268.
[69] Sakaue-Sawano A, Kobayashi T, Ohtawa K, and Miyawaki A (2011). Drug-induced cell cycle modulation leading to cell-cycle arrest, nuclear mis-segregation, or endoreplication. *BMC Cell Biol* **12**, 2.